Preparation and Characterization of Sepiolite-Poly(ethyl methacrylate) and Poly(2-hydroxyethyl methacrylate) Nanocomposites

Ruhan Benlikaya,[1] Mahir Alkan,[2] İsmet Kaya[3]
[1]*Department of Secondary Science and Mathematics Education, Balikesir University, Balikesir, Turkey*

[2]*Department of Chemistry, Balikesir University, Balikesir, Turkey*

[3]*Department of Chemistry, Çanakkale Onsekiz Mart University, Çanakkale, Turkey*

Poly(ethyl methacrylate) (PEMA) and poly(2-hydroxyethyl methacrylate) (PHEMA) nanocomposites with sepiolite in pristine and silylated form were prepared using the solution intercalation method and characterized by the measurements of XRD, TEM, FTIR-ATR, TG/DTG, and DSC. The TEM analysis indicated that the volume fraction of fibers in sepiolite decreased and the fiber bundles dispersed in PEMA and PHEMA at a nanometer scale. These results regarding TEM micrographs were in agreement with the data obtained by XRD. The increase in thermal stability of nanocomposites of PEMA is higher than that of PHEMA according to the data obtained from TG curves. The DTG analysis revealed that sepiolite/modified sepiolite caused some changes, as confirmed by FTIR in the thermal degradation mechanism of the polymers. T_g temperatures of PEMA and PHEMA usually increased upon the addition of sepiolite/modified sepiolite. In addition, modification of sepiolite with 3-APTS had a slight influence on thermal properties of the nanocomposites. POLYM. COMPOS., 30:1585–1594, 2009. © 2008 Society of Plastics Engineers

INTRODUCTION

The term "nanocomposite material" has attracted great interest in recent years for exhibiting remarkable improvement in mechanical properties, barrier properties, thermal properties, optical properties, and ionic conductivity and is commonly used in two distinct areas of material science such as ceramics and polymers [1, 2]. Particles (silica, metal, and other organic and inorganic materials), layered materials (graphite, layered silicate, and other layered minerals), and fibrous materials (nanofibers and nanotubes) are used as reinforcement materials in polymer nanocomposites [3].

The commonly used layered silicates for the preparation of polymer-layered silicate nanocomposites belong to the same general family of 2:1 (T:O:T) layered silicates or phyllosilicates. While montmorillonite (MMT), hectorite, and saponite are the most commonly used layered silicates [1], few reports concerning sepiolite, is displayed by the structural formula ($Mg_8[(OH)_2/Si_{12}O_{30}] \cdot 4H_2O + 8H_2O$), have been encountered in the literature. Sepiolite has a structure similar to the 2:1 layered structure of MMT formed by two tetrahedral silica sheets enclosing a central sheet of octahedral magnesia except that the layers lack continuous octahedral sheets [4]. There are channels and tunnels in the structure of sepiolite and it has fibrous morphology, because each T:O:T linked to the next by inversion SiO_4 tetrahedra a long a set of Si—O—Si bonds [5]. The presence of silanol groups (Si—OH) at the edges of the tunnels can enhance the interfacial interaction between sepiolite and polymer. These can induce certain amount of sepiolite dispersed at the nanometer scale in polymer matrix and improve the mechanical and thermal properties of polymers [6]. In addition, the exchange capacity of sepiolite is less than that of smectites (20–60 meq) but their significant capacity to absorb organic molecules has led to their use as industrial and domestic absorbant [5]. This is why so many adsorption studies relating to sepiolite were conducted [7–11].

The polymers used as a matrix in the studies of the nanocomposites containing sepiolite are Nylon-6 [4], polyurethane [6], poly(hydroxyethyl acrylate) [12], poly (sodium acrylate) [13], chitosan [14], epoxy resin [15, 16], poly(dimetylsiloxane) [17, 18], polyester [19], and polypropylene [20, 21]. Nanofibers of sepiolite ensure the

Correspondence to: R. Benlikaya; e-mail: ruhan@balikesir.edu.tr
Contract grant sponsor: Balikesir University; contract grant number: 2006/01.
Contract grant sponsor: TUBITAK; contract grant number: 106T453.
DOI 10.1002/pc.20731
Published online in Wiley InterScience (www.interscience.wiley.com).

substantial improvements in the mechanical properties [12, 14, 15, 17–19] and thermal stability [11, 14, 16] of these polymers even at low filler loadings. Also carbon nanofibers [22] and carbon-silicates [23] are produced through graphitization of poly(acrylonitrile) [22] and of sucrose [23] inside the nanosized pores of sepiolite.

Poly(*n*-alkyl methacylate)s, (PaMA)s, consist of a polar backbone and usually flexible nonpolar sidegroups $R_n = C_nH_{2n+1}$. Owing to their excellent properties (high transparency, light weight, good mechanical, and electrical properties etc.), poly(alkyl methacrylate)s are used in architecture, industry, motorization, agriculture, medicine, pharmacy, as well as in the textile, paper, and paint industries [24]. In this study, poly(ethyl methacrylate) (PEMA) and poly(2-hydroxyethyl methacrylate) (PHEMA) were selected as matrix to prepare the nanocomposites.

In the studies where PEMA was used as a matrix, the nanocomposites of montmorillonite [25], dibenzylidene sorbitol/colloidal silica [26], and $FeCl_3$ [27] were prepared using the solution intercalation method. As to the studies related to PHEMA nanocomposites, (DMSO)(MeOH)-Cu_2(benzene-1,3-dicarboxylate-5-OH)$_2I_{12}$ [28] in polymerization medium, silica [29] and TiO_2 [30] in sol-gel process and silica [29] in direct mixing were used as fillers.

As can be seen above, no nanocomposite study relating to these PaMAs with sepiolite has been reported so far in the literature. In this study, PEMA and PHEMA nanocomposites with sepiolites in pristine and silylated form were prepared through the solution intercalation method. The method was used to give a good control on the homogeneity of constituents [25]. For characterization of the nanocomposite samples, the measurements of FTIR, XRD, TEM, TG/DTG, and DSC were used. It was also investigated whether there was any influence of modification of sepiolite with 3-aminopropyltriethoxylsilane (3-APTS) and of side group in PaMAs on the properties of the nanocomposites.

EXPERIMENTAL

Materials

Sepiolite (JCPDS 29-1492) was provided from Aktaş Lületaşı corporation, in Eskişehir, Turkey. All the chemicals in the study were analytical grade and used without further purification. PEMA and PHEMA were obtained commercially from Across and Aldrich. The 3-APTS, ethanol, and diethyl ether were from Aldrich, Carlo Erba, and Merck, respectively.

Modification of Sepiolite

Sepiolite was oven-dried, ground, and sieved to a size of ~75-μm diameter. Then, sepiolite was modified with 3-aminopropyl triethoxyl silane (3-APTS) according to synthesis route described in a previous paper [6]. In this study, for modification the surface polarity of sepiolite 3-APTS was used taking into consideration the structure of the polymers and solvents (or mixtures). Sepiolite modified with 3-APTS involves both of the polar and apolar sides which can interact with PEMA and PHEMA chains.

Preparation of Sepiolite and Modified Sepiolite/ Polyalkylmethacrylate Nanocomposites

Sepiolite was dispersed in organic solvents, which were diethyl ether-ethyl alcohol mixture (1:1) with a solubility parameter of $\delta = 20.8$ MPa$^{1/2}$ for PEMA ($\delta = 20.5$) and ethyl alcohol ($\delta = 26.2$) for PHEMA ($\delta = 26.9$) [31], using a magnetic stirrer for 2 h at room temperature followed by ultrasonic treatment for 20 min to gain a uniform dispersion of sepiolite fillers. Then, the polymers were added to the corresponding suspensions. After dissolving, the mixtures were stirred for a 24 h. The samples were poured into glass petri dishes and they were evaporated at 40°C in an oven. The same method was also applied to modified-sepiolite. The obtained products were identified as SepPHEMA, ModsepPHEMA, etc.

Measurement

FTIR measurements were performed with a Perkin Elmer Spectrum One FTIR with ATR for scanning coverage from 650 to 4,000 cm^{-1}. XRD patterns were obtained using Rigaku Rint 2000 diffractometer. X-ray beams were derived from nickel-filtered Cu Kα ($\lambda = 0.154$ nm) radiation in a sealed tube operated at 40 kV, 30 mA, and the diffraction curves were obtained from 5 to 50 at a scan rate of 0.02°/min. Transmission electron microscopy (JEOL JEM 2100) was used to determine the morphologies of sepiolite and the composites at an acceleration voltage of 200 kV. For the TEM study, the sample taken from sepiolite having been dispersed in ethanol through ultrasonic treatment and the samples of polymer-sepiolite suspensions were deposited on a 200-mesh copper grid.

The thermal stabilities of the nanocomposites were investigated by using a Perkin Elmer Pyris Diamond TG/DTA. The TG scans were recorded at a temperature ramp of 10°C/min under constant nitrogen flow of 200 ml/min from 60 to 600°C. DTG curves were used to investigate if a change occurred in thermal degradation mechanism of PEMA and PHEMA. Glass transition temperatures were investigated at a temperature ramp of 20°C/min in nitrogen flow from 50 to 200°C by Perkin Elmer Sapphire DSC. The temperatures were determined as the midpoints of reverse "*S*" shaped thermograms.

RESULTS AND DISCUSSION

FTIR and XRD for Modification of Sepiolite

Figure 1 depicts FTIR-ATR spectra of raw sepiolite and modified sepiolite. The bands of OH deformation at

 DOI 10.1002/pc

979 cm^{-1} shifted to higher wavelengths and OH translation at 781 and 680 cm^{-1} shifted to lower wavelengths after the modification of sepiolite. The area of the bands between 3,000 and 4,000 cm^{-1} assigned to the —OH stretching vibrations decreased after modification by 3-APTS. The new bands attributed to C—H bond of $—CH_2$ between 2,900 and 3,000 cm^{-1} were observed in FTIR of modified sepiolite as shown in Fig. 1. These findings indicated that a chemical reaction [6] occurred during the modification as shown in *Eq. 1*.

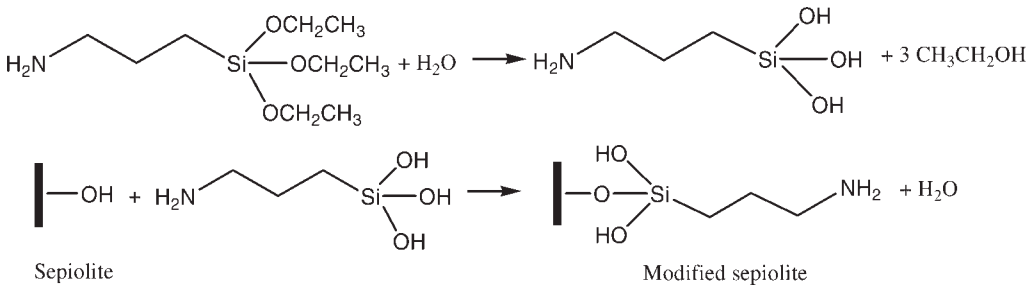

(1)

The XRD pattern of sepiolite used in this study showed the characteristic 110 peak of sepiolite at 1.23 nm ($2\theta = 7.2^\circ$) and existence of magnesite ($2\theta = 32.56^\circ$, JCPDS 8-479) as impurity as can be seen in Fig. 2. As sepiolite is a non-swelling clay, organophilization occurs mainly through a surface modification, maintaining its crystalline structure. However, the organic modification can decrease the aggregation of fibers and result in a weak diffraction peak [6]. In our study, a decrease was observed in the intensity of the 110 peak as shown in Fig. 2.

Characterization of Nanocomposites

Nanocomposites of PEMA and PHEMA with raw sepiolite and modified sepiolite were prepared in concentrations of 2.5 and 5% of sepiolite.

XRD. The XRD patterns for PEMA and PHEMA and their nanocomposites with sepiolite and modified sepiolite were shown in Figs. 3 and 4. As shown in these figures, the disappearance of the 110 peak of sepiolite in XRD patterns of PEMA and PHEMA with sepiolite/modified sepiolite composites, except SepPEMA 5%, was considered as an evidence for highly dispersion of sepiolite fibers. The intensity of 110 peak is related to the volume fraction of sepiolite fibers, i.e., the lower the volume fraction of fibers reduce, the weaker the diffraction peak will be [6]. For SepPEMA 5%, a relatively small diffraction peak displayed at $2\theta = 7.2^\circ$. This was probably a consequence of increase in the volume fraction, which is the indication of the agglomeration of some sepiolite fibers. This small diffraction peak for SepPEMA5% was not observed for ModsepPEMA5%. This showed that the modified sepiolite was dispersed in PEMA better than unmodified sepiolite because the modifying agent, 3-APTS, improved the interaction of surface with poly(ethyl methacrylate).

TEM. Transmission electron microscopy (TEM) analysis can provide more direct evidence for the formation of

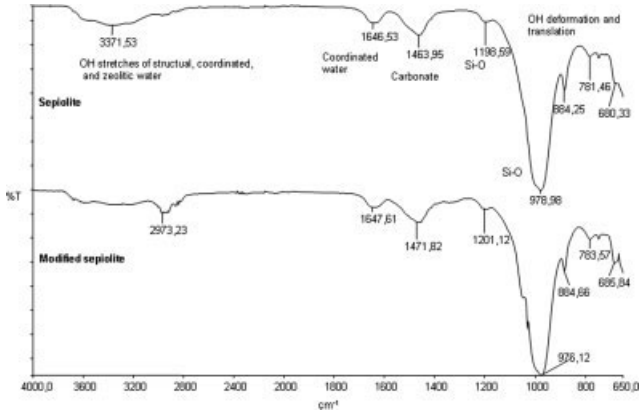

FIG. 1. FTIR spectra of sepiolite and modified sepiolite.

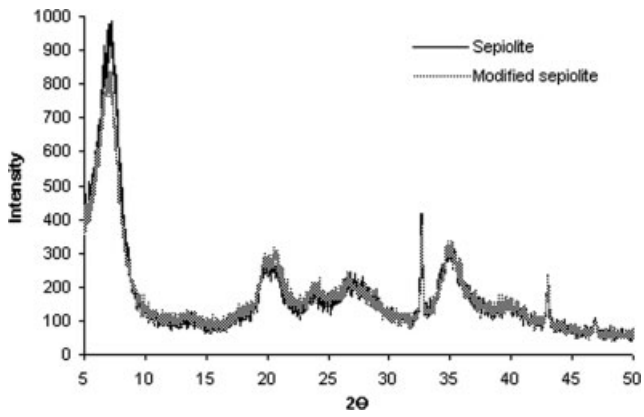

FIG. 2. XRD patterns of sepiolite and modified sepiolite.

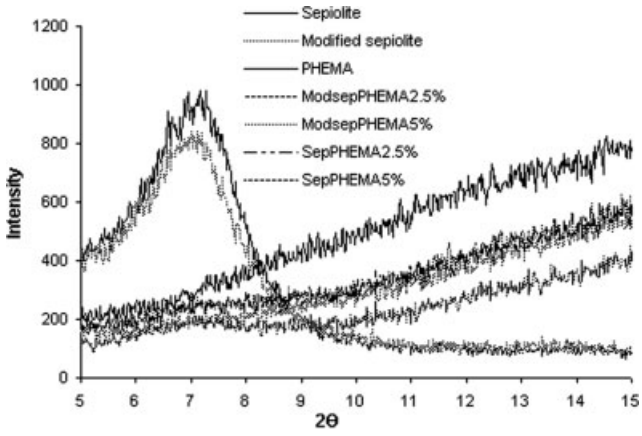

FIG. 3. XRD patterns of pure PHEMA and its nanocomposites.

nanocomposites. TEM micrographs were obtained for sepiolite, modified sepiolite, and composites with the fillers loading 2.5%. The fibrous morphology of sepiolite/modified sepiolite is also confirmed by Fig. 5a and b. The diameter of the single fiber was measured as 10–12 nm. While it was observed that the approximate diameter (AD) of the fiber bundles in sepiolite was between 100 and 350 nm, the range decreased to 60–250 nm in modified sepiolite. As shown in Fig. 5c and d, the volume fraction of fibers (or the thickness of clay laths) in the PHEMA composites decreased in comparison to the image for sepiolite/modsepiolite in Fig. 5a and b and the fiber bundles (AD: 30–60 nm) dispersed in the matrix at a nanometer scale. The presence of those structures was also observed in palygorskite-epoxy polymer system [32]. In the case of PEMA composites, it was observed that some fiber bundles interconnected with each other as can be seen in Fig. 5e and f, in addition to the structures observed in the TEM images Fig. 5e of PHEMA nanocomposites. In additionally these results relating to TEM micrographs were in agreement with the data obtained by XRD.

FTIR-ATR Spectra. FTIR-ATR studies were usually carried out to understand possible chemical and physical interactions between sepiolite/modified sepiolite and PEMA/PHEMA. Figure 6 shows FTIR specta of PEMA and PHEMA and their composites with sepiolite/modified sepiolite. The carbonyl stretching vibration at around 1,700 cm^{-1} in spectra of PEMA and PHEMA was shifted to lower wavelengths in their composites except modsep-PEMA 2.5%. The shift in PHEMA was more than PEMA. The stretches of $—CH_3$, asymmetric $—CH_2$ and aliphatic —CH at around 2,900 cm^{-1} in PHEMA were shifted to lower wavelengths, while they remained almost unchanged in PEMA. The results can be attributed to the weak Van der Walls interactions occurring between PEMA and sepiolite surface. As can be understood from the molecular structure of PEMA in Fig. 7 only Van der Walls interactions can take place during the preparation of polymer nanocomposites.

The —OH band at 3,381 cm^{-1} was shifted to lower wavelengths in their composites with sepiolite/modified sepiolite and the hydrogen bonds in PHEMA [33], as illustrated in Fig. 7, weakened in the composites due to the interactions between —SiOH group at the external surface of sepiolite, ester and —OH group in PHEMA.

The bands around 1,550–1,300 cm^{-1} were caused by the $—CH_3$ and $—CH_2$ deformations and the absorptions in the 1,300–1,000 cm^{-1} region by the C—O—C stretching vibrations in PEMA and PHEMA. Some differences were observed in the C—O—C stretching vibrations of the composites. While the band at around 1,030 cm^{-1} in both of PEMA and PHEMA was disappeared in the composites, the new band between 1,200 and 1,230 cm^{-1} appeared in PHEMA's composites.

The above analysis indicated clearly that these matrixes and sepiolite/modified sepiolite were not simply blended but also complex interactions exist between them.

Thermal Properties of Nanocomposites. *TG/DTG Measurements.* The thermal stabilities of the composites were investigated using a thermo-gravimetric analyzer. Figures 8 and 9 shows the TG and DTG curves of PEMA and PHEMA and their composites. Thermal stabilities of the samples were determined by considering the degradation temperatures at 5, 10, 50, and 80% weight losses obtained from the TG curves. These values are shown in Table 1. It is a well known fact that the higher the value of the degradation temperatures increases, the higher the thermal stability is.

The data obtained from the TG curves shown in Figs. 8a and 9a demonstrate that the thermal stability of the prepared nanocomposites was better than that of the pure PEMA and PHEMA. The incorporation of sepiolite into these polymers was found to enhance thermal stability. This finding may be result of two reasons: (i) sepiolite may act as a superior insulator and a mass transport barrier to the volatile products generated during decomposition as observed MMT-polymer nanocomposites [1]. This effect may not be as important for sepiolite nanocomposites as being the MMT nanocomposites, because sepiolite

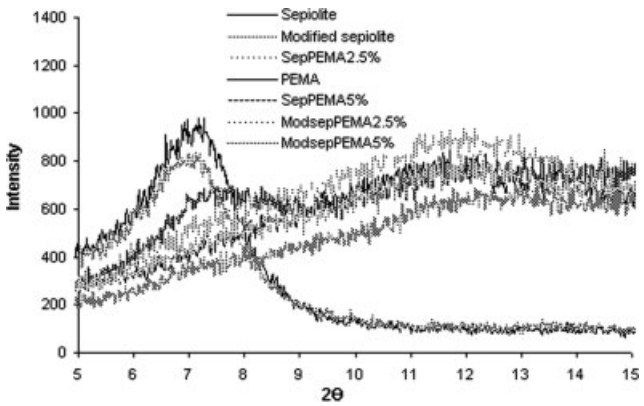

FIG. 4. XRD patterns of pure PEMA and its nanocomposites.

DOI 10.1002/pc

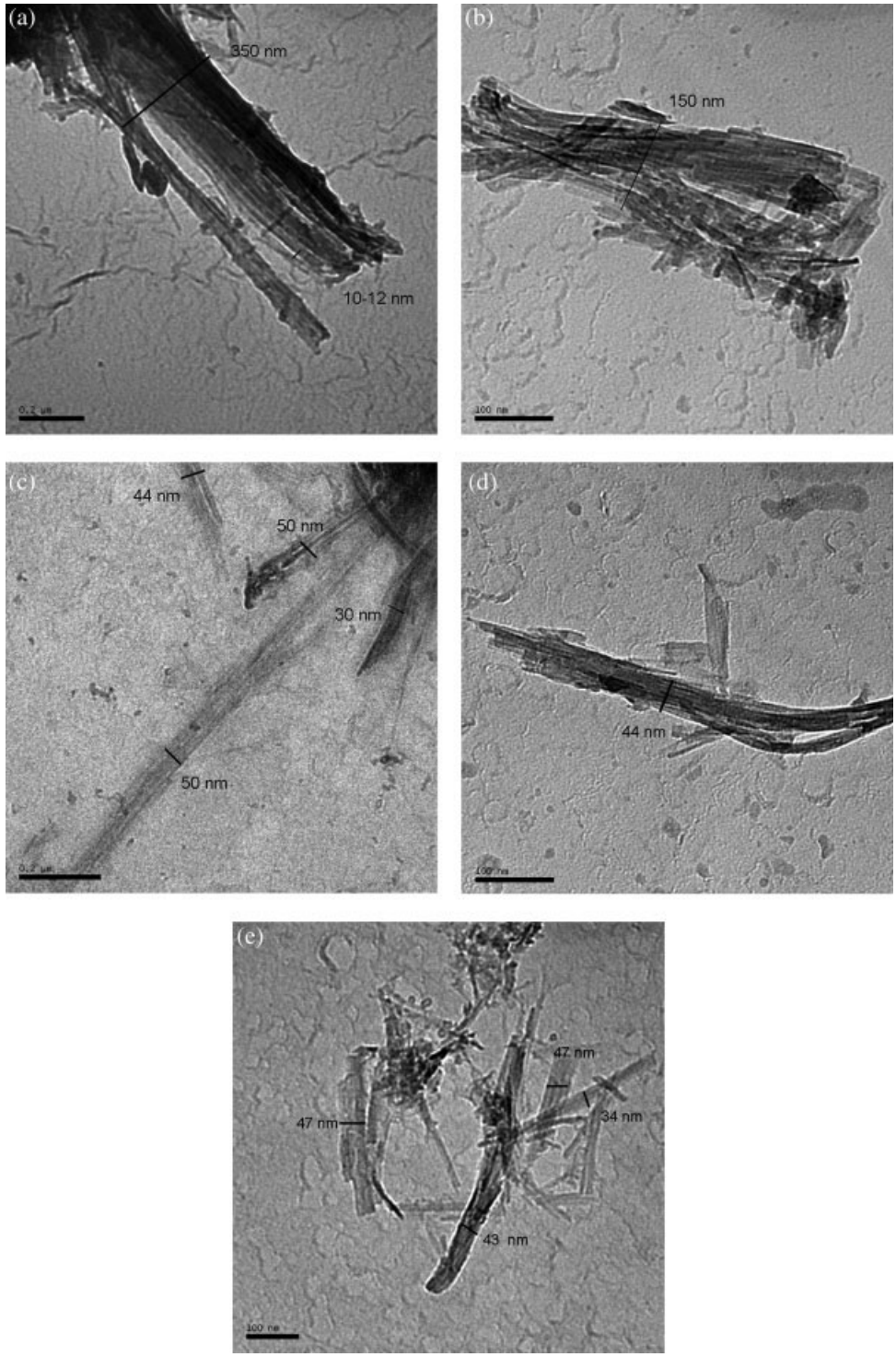

FIG. 5. TEM images of sepiolite (a), modified sepiolite (b), PEMA and PHEMA nanocomposites with them (c, d, e).

is a needle like shaped clay while MMT is a platelet-like. (ii) Sepiolite acts as a "crosslinking agent" retarded the motion of the polymer chains [6]. It was observed that the increase in thermal stability for PEMA was higher than that of PHEMA. The addition sepiolite into PHEMA got the interactions of polymer chains weaker than those occurred in the case of PEMA.

When the loading effect was considered, it was found that the thermal stability of PEMA nanocomposites increased with loading percent of modified sepiolite, but it decreased in the case of unmodified sepiolite loading percent. The effect of sepiolite on the thermal stability is expected to increase with improving the degree of dispersion of sepiolite. For SepPEMA5%, the degree

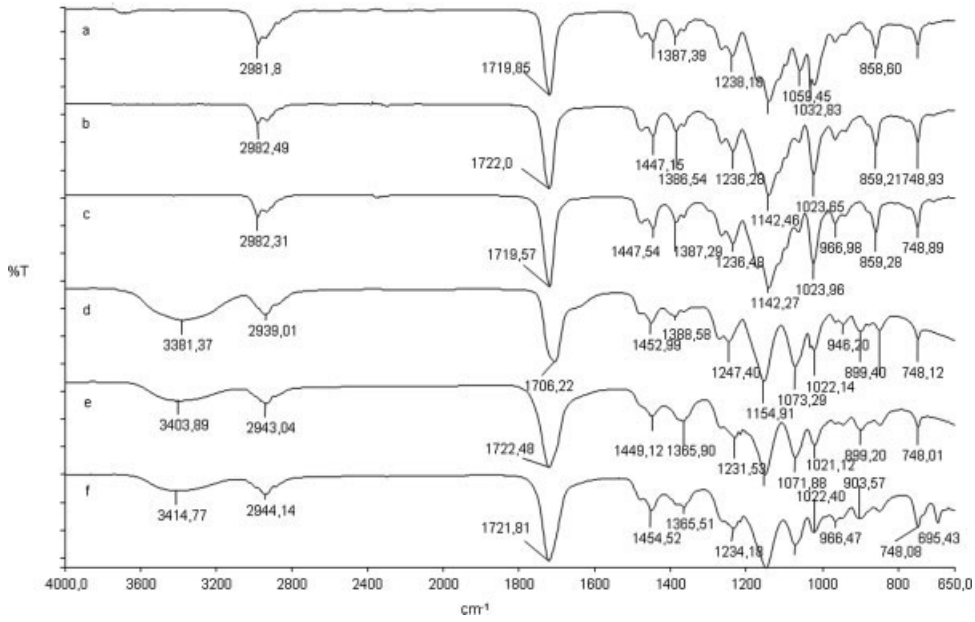

FIG. 6. FTIR spectra of pure PEMA, PHEMA and their composites: (a) PEMA, (b) SepPEMA2.5%, (c) ModsepPEMA2.5%, (d) PHEMA, (e) SepPHEMA2.5%, (f) ModsepPHEMA2.5%.

of dispersion is not so high as in SepPEMA2.5% because of agglomeration observed in XRD pattern of SepPEMA5%.

In the case of PHEMA, as the loading percentage of sepiolite/modified sepiolite in the nanocomposites increased, the thermal stability of PHEMA nanocomposites also increased, albeit slightly. No significant difference was found in the thermal properties of sepiolite and modified sepiolite with 3-APTS nanocomposites.

In addition, as given in Table 1, the char yield increased in line with the amount of sepiolite and modified sepiolite and this enhancement of the char formation was ascribed to the high heat resistance exerted by them.

Thermal degradation of poly-*n*-alkyl methacrylates (PAMAs) produces monomers as a result of depolymerization, which is the main reaction in this degradation process. The formation of poly(methacrylic acid) is also a characteristic process in PAMAs' thermal degradation at high temperature except poly(methyl methacrylate). The degradation products are of low molecular weight and their composition depends on the chemical structure of

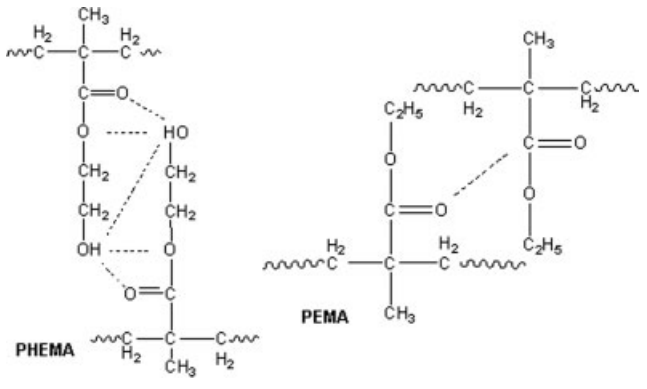

FIG. 7. The interactions in PEMA and PHEMA.

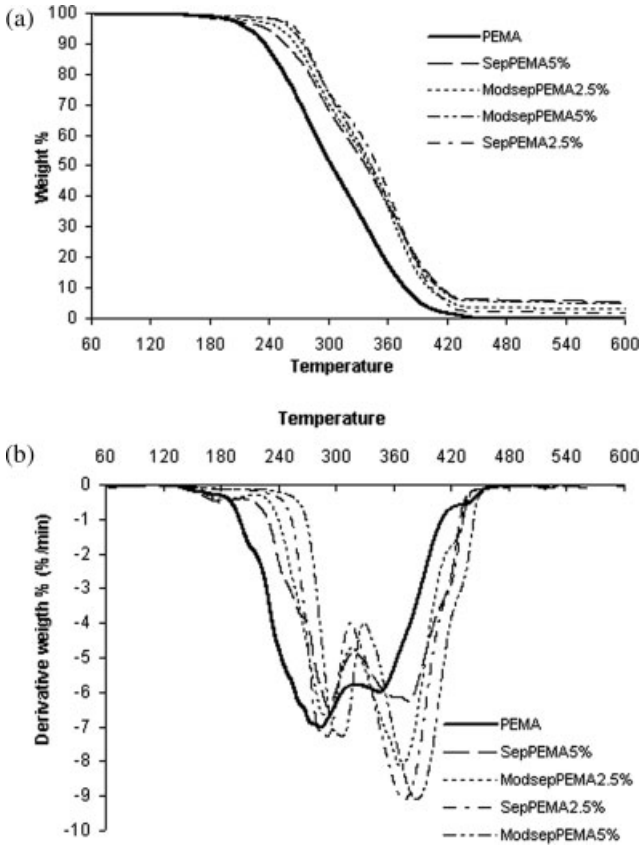

FIG. 8. TG (a) and DTG (b) curves of pure PEMA and its nanocomposites.

DOI 10.1002/pc

the side chain of the polymer [34, 35]. Pyrolysis studies of PEMA [36, 37] and PHEMA [38–40] show that the degradation of these polymers is very similar at least in the initial stage which is monomer evolution step. The reactions involving initial cleavage of head-to-head linkages and β-scission at vinylidene chain ends followed by unzipping occurred in the initial stages to about 300°C were shown in *Eqs. 2* and *3* [39].

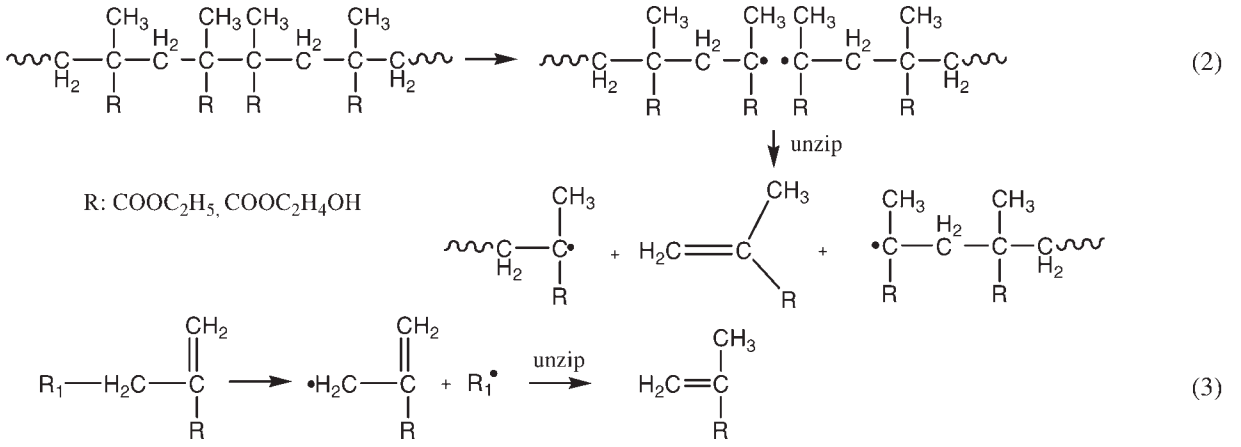

(2)

(3)

According to our results given in Fig. 8b, after the initial stages the formation of poly(methacrylic acid) (~250–350°C), the formation of anhydride structures (~350–420°C) and the degradation of the polymer itself by the decomposition of the partially degraded backbone carrying anhydride groups [35] (~420–500°C) occurred in the degradation of PEMA. In the case of PHEMA, the reactions from about 300–500°C included the formation of poly(methacrylic acid), poly(methacrylic anhydride)s, ethylene glycol, and ethylene glycol dimethacrylate [40]. The reactions involve main products (a–d) in the degradation of PEMA and PHEMA after the initial stages were shown in *Eq. 4* and *5* [39–42].

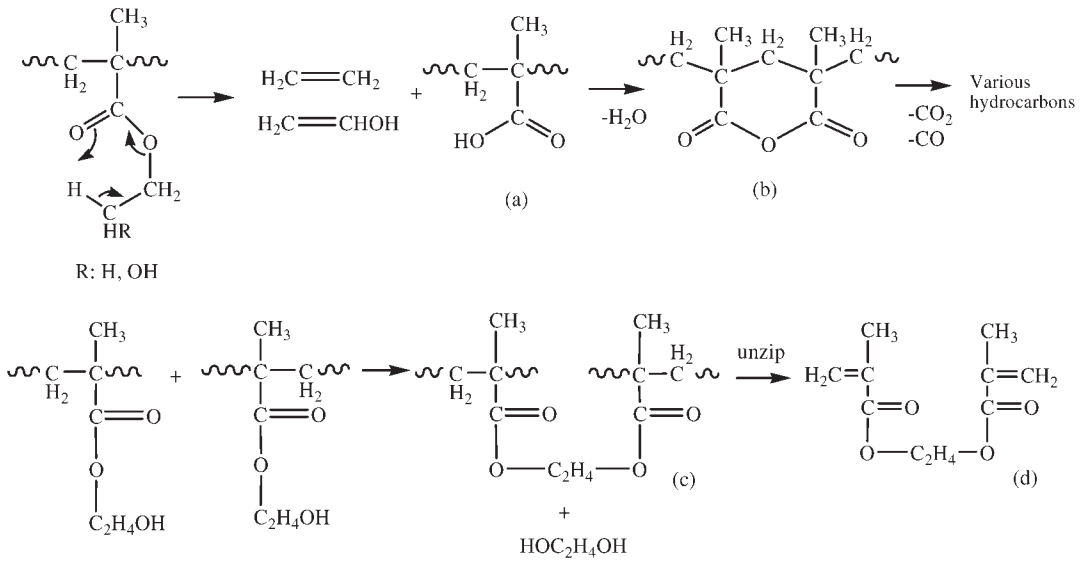

(4)

(5)

* In addition to the product with labelled (b), other anhydride structures can also be formed [40-42].

The DTG thermograms revealed that sepiolite/modified sepiolite produced the changes in the thermal degradation mechanisms of the polymers. For SepPEMA nanocomposites, the shift of the right shoulder in DTG curve of PEMA to higher temperature and broadening in the peak related to the formation of anhydride structure was

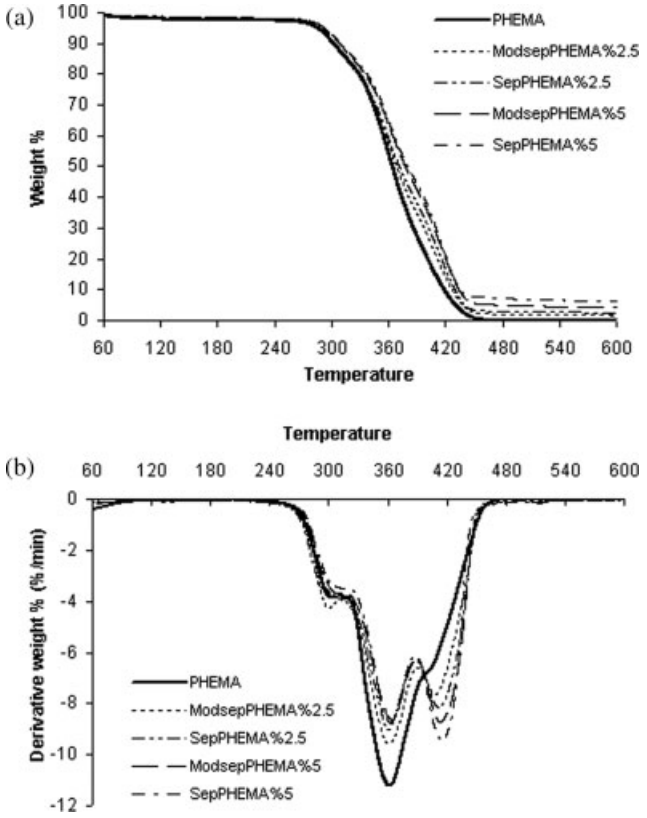

FIG. 9. TG (a) and DTG (b) curves of pure PHEMA and its nanocomposites.

observed in DTG thermograms of PEMA composites as shown in Fig. 8b. In the case of PHEMA composites, the distinct peak which was not observed in PHEMA at around 420°C was identified in the DTG curves, as can be seen Fig. 9b.

TABLE 1. The data obtained from TG and DSC curves of the polymers and their nanocomposites.

System	T_5 (°C)[a]	T_{10} (°C)	T_{50} (°C)	T_{80} (°C)	Char (%)	T_g (°C)[b]
PEMA	217	235	303	356	~0	64
Sep-PEMA 2.5%	266	276	349	386	1.9	70
Sep-PEMA 5%	237	256	338	389	5.6	67
Modsep-PEMA 2.5%	251	267	341	381	3.3	72
Modsep-PEMA 5%	262	273	343	387	5.2	73
PHEMA	286	301	364	401	~0	92
Sep-PHEMA 2.5%	286	301	371	415	2.6	90
Sep-PHEMA 5%	292	309	380	421	6.3	104
Modsep-PHEMA 2.5%	288	301	368	411	1.7	96
Modsep-PHEMA 5%	292	308	378	420	4.4	99

[a] The temperature for 5% weight loss.
[b] The temperature of glass transition.

Infrared spectra of residues at various temperatures (360, 400, 420, and 450°C) were studied to understand the observed differences in the DTG curves. Important differences were observed at 420°C as shown in Fig. 10. While poly(methacrylic acid), shown as in *Eq. 4* and Fig. 10, was still observed at 420°C in PHEMA nanocomposites, it did not appear in PHEMA. This finding showed that the decomposition rate of poly(methacrylic acid) decreased in the presence of sepiolite. In respect of the FTIR spectra of the residues of PEMA and its nanocomposites at 420°C, no difference was found in the formation of poly(methacrylic acid). But the appearance of the band related to carbon dioxide at around 2,350 cm^{-1} and of a decrease in the intensity of the peaks between 1,750 and 1,800 cm^{-1} in FTIR spectra of PEMA nanocomposites showed that the decomposition of anhydride structures (b) advanced more rapidly than PEMA. The fact

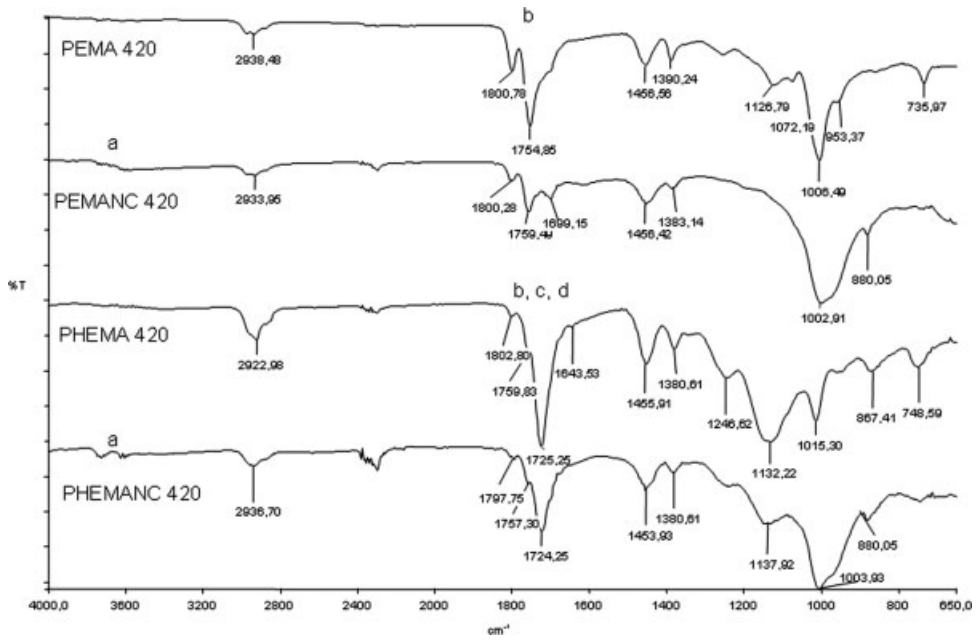

FIG. 10. FTIR spectra for the residues of PEMA, PHEMA, and their nanocomposites (NC) at 420°C.

 DOI 10.1002/pc

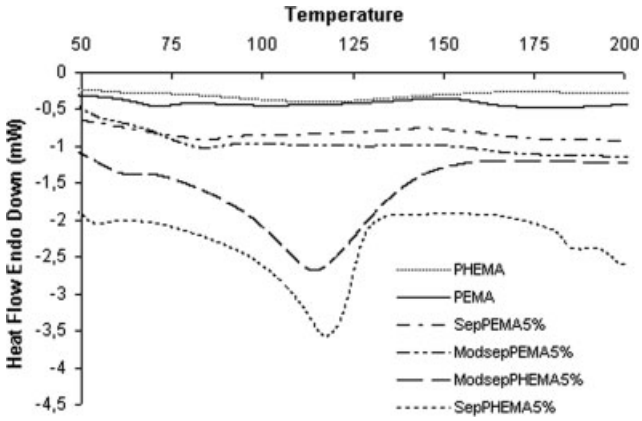

FIG. 11. DSC curves of pure PEMA, PHEMA and their nanocomposites with sepiolite/modsepiolite (5 wt%).

that the bands between 800 and 1,200 cm^{-1} for both of poly(ethyl methacrylate) and poly(2-hydroxyethyl methacrylate) were different in comparison to their nanocomposites confirmed the changes in DTG curves of nanocomposites.

DSC Measurements. Glass transition (T_g) temperatures of poly(ethyl methacrylate), poly(2-hydroxyethyl methacrylate) and their composites were measured from DSC curves shown in Fig. 11 and the obtained values are shown in Table 1. T_g temperatures of PEMA and PHEMA usually increased by adding sepiolite/modified sepiolite, as can be seen from Fig. 11 and Table 1. The result indicated that the mobility of these polymers molecules was restricted by the dispersed sepiolite/modified sepiolite.

CONCLUSIONS

Solution intercalation method was used to prepare poly(ethyl methacrylate) and poly(2-hydroxyethyl methacrylate) composites with sepiolite in pristine and silylated form. The composites were characterized by XRD, TEM, FTIR, TG/DTG, and DSC. The data obtained from XRD and TEM indicated that the fibers of sepiolite dispersed in matrix at a nanometer scale and their volume fractions decreased in the composites, confirming the formation of nanocomposite.

When the difference in the interactions between PEMA/PHEMA and sepiolite/modsepiolite was investigated by FTIR data, it was observed that Van der Walls forces in PEMA and hydrogen bonding in PHEMA can be effective during the preparation of nanocomposites with sepiolite/modified sepiolite. The increase in thermal stability of nanocomposites for PEMA was higher than that of PHEMA because of the weakening hydrogen bonds in PHEMA in the presence of sepiolite/modsepiolite. In addition, the DTG analysis revealed that sepiolite/modified sepiolite caused some changes in thermal degradation mechanisms of the polymers as confirmed by FTIR. According to the DSC curves, the T_g temperatures of PEMA and PHEMA usually increased by adding sepiolite/modified sepiolite. There was no relationship between the increase in thermal stability/T_g temperatures and amount of the fillers.

Modification of sepiolite with APTS had a slight influence on thermal properties of the nanocomposites. Merely the modified sepiolite dispersed in PEMA better than the unmodified sepiolite according to the XRD and TG data because the modifying agent, 3-APTS, improved the interaction of surface with PEMA.

REFERENCES

1. S.S. Ray and M. Okomoto, *Prog. Polym. Sci.*, **28**, 1539 (2003).
2. X. Kornmann, *Synthesis and Characterization of Thermoset-Clay Nanocomposites: Introduction*, Lulea Tekniska Universite, Lulea (1999).
3. E.T. Thostenson, C. Li, and T. Chou, *Compos. Sci. Tech*, **65**, 491 (2005).
4. S. Xie, S. Zhang, F. Wang, M. Yang, R. Séguéla, and J.-M. Lefebvre, *Compos Sci and Technol*, **67**, 2334 (2007).
5. B. Velde, *Introduction to Clay Minerals: Chemistry, Origins, Uses and Environmental Significance*, Chapman & Hall, London (1992).
6. H. Chen, M. Zheng, H. Suna, and O. Jia, *Mater. Sci. Eng. A*, **15**, 725 (2007).
7. N. Tekin, A. Dinçer, Ö. Demirbaş, and M. Alkan, *J. Hazar. Mater.*, **134(1–3)**, 211 (2006).
8. M. Alkan, M. Doğan, Y. Turhan, Ö. Demirbaş, and P. Turan, *Chem. Engin. J.*, **139(2)**, 213 (2008).
9. S. Balci, *Water Res.*, **38(5)**, 1129 (2004).
10. O. Özdemir, M. Çınar, E. Sabah, F. Arslan, and M.S. Çelik, *J. Hazar. Mater.*, **147(1/2)**, 625 (2007).
11. Ö. Demirbaş, M. Alkan, M. Doğan, Y. Turhan, H. Namli, and P. Turan, *J. Hazar. Mater.*, **149(3)**, 650 (2007).
12. L. Bokobza, A. Burr, G. Garnaud, My. Perin, and S. Pagnotta, *Polym. Int.*, **53**, 1060 (2004).
13. F. Santiago, A.E. Mucientes, M. Osorio, and F.J. Poblete, *Polym. Int.*, **55**, 843 (2006).
14. M. Darder, M. Lopez-Blanco, P. Aranda, A.J. Aznar, J. Bravo, and E. Ruiz-Hitzky, *Chem. Mater.*, **18**, 1602 (2006).
15. Y. Zheng and Y. Zheng, *J. Appl. Polym. Sci.*, **99**, 2163 (2006).
16. A. Toldy, N. Toth, Gy. Keglevich, K. Kiss, and Gy. Marosi, *Polym. Adv. Technol.*, **17**, 778 (2006).
17. F.-X. Deneuborg, A. Beigbeder, Ph. Degee, and P. Viville, Ph Dubois. Silicone-Based Nanocomposites: New Materials for Antifouling Coatings. Available at: http://morris.umh.ac.be/SMPC/Posters/2006-BPG-FRDE.pdf.
18. L. Bokobza, *J. Appl. Polym. Sci.*, **93**, 2095 (2004).
19. E. Duquesne, S. Moins, M. Alexandre, and P. Dubois, *Macromol. Chem. Phys.*, **208**, 2542 (2007).
20. J. Ma, E. Bilotti, T. Peijs, and J.A. Darr, *Eur. Polym. Sci.*, **43(12)**, 4931 (2007).
21. E. Bilotti, H.R. Fischer, and T.J. Peijs, *Appl. Polym. Sci.*, **107(2)**, 1116 (2008).

22. A. Gomez-Aviles, M. Darder, P. Aranda, and E. Ruiz-Hitzky, *Angew. Chem. Int. Ed.*, **45**, 1 (2006).
23. R. Fernandez-Saavedra, P. Aranda, and E. Ruiz-Hitzky, *Adv. Funct. Mater.*, **14**, 77 (2004).
24. H.F. Mark, *Encyclopedia of Polymer Science and Engineering*, Wiley, New York (1985).
25. Y. Li and H. Ishida, *Polymer*, **44**, 6571 (2003).
26. E.A. Wilder, M.B. Braunfeld, H. Jinnai, C.K. Hall, D.A. Agard, and R.J. Spontak, *J. Phys. Chem. B*, **107**, 11633 (2003).
27. E.M. Abdelrazek, *Phys. Rev. B: Condens. Matter*, **400**, 26 (2007).
28. K. Mohomed, T.G. Gerasimov, H. Abourahma, M.J. Zaworotko, and J.P. Harmon, *Mater. Sci. Eng. A*, **409**, 227 (2005).
29. S.-L. Huang, W.-K. Chin, and W.P. Yang, *Polymer*, **46**, 1865 (2005).
30. K. Prashanta, B.J. Rashmi, T.V. Venkatesha, and J.-H. Lee, *Spectrochim. Acta A*, **65**, 340 (2006).
31. J. Burke, AIC Book and Paper Group International 1984; 13, Available at: http://sul-server-2.stanford.edu/byauth/burke/solpar/.
32. S. Xue, M. Reinholdt, and T.J. Pinnavia, *Polymer*, **47**, 3344 (2006).
33. D.J.T. Hill, J.H. Odenell, P.J. Pomery, and G. Saadat, *Radiat. Phys. Chem.*, **48**, 605 (1982).
34. M. Coşkun, K. Demirelli, I. Erol, and M. Ahmedzade, *Polym. Degrad. Stab.*, **61**(**3**), 493 (1998).
35. F. Bertini, G. Audisio, and V.V. Zuev, *Polym. Degrad. Stab.*, **89**, 233 (2005).
36. B. Işık-Yürüksoy, S. Şenel, and O. Güven, *J. Therm. Anal.*, **48**(**4**), 783 (1997).
37. S.L. Malhotra, Ly. Minh, and L.P. Blanchard, *J. Macromol. Sci. Pure Appl. Chem.*, **19**(**4**), 559 (1983).
38. J. Razga and J. Petranek, *Eur. Polym. J.*, **11**, 805 (1975).
39. M. Thekkekalathill, T.M. Chandrasekhar, and R.L. White, *J. Appl. Polym. Sci.*, **60**, 1209 (1996).
40. K. Demirelli, M. Coskun, and E. Kaya, *Polym. Degrad. Stab.*, **72**, 75 (2001).
41. M. Lazzari, T. Kitayama, and K. Hatada, *Macromolecules*, **31**, 8075 (1998).
42. B.-C. Ho, Y.-D. Lee, and W.-K. Chin, *J. Polym. Sci. Part A: Polym. Chem.*, **30**, 2389,(1992).

 DOI 10.1002/pc